

See discussions, stats, and author profiles for this publication at: <https://www.researchgate.net/publication/224877649>

# Effect of Nitrogen Doping on Hydrogen Storage Capacity of Palladium Decorated Graphene

ARTICLE *in* LANGMUIR · MAY 2012

Impact Factor: 4.46 · DOI: 10.1021/la301232r · Source: PubMed

---

CITATIONS

65

READS

328

## 3 AUTHORS:



B P Vinayan

Helmholtz-Institut Ulm

32 PUBLICATIONS 505 CITATIONS

[SEE PROFILE](#)



Rupali Nagar

Symbiosis Institute of Technology

21 PUBLICATIONS 444 CITATIONS

[SEE PROFILE](#)



Ramaprabhu Sundara

Indian Institute of Technology Madras

57 PUBLICATIONS 1,121 CITATIONS

[SEE PROFILE](#)

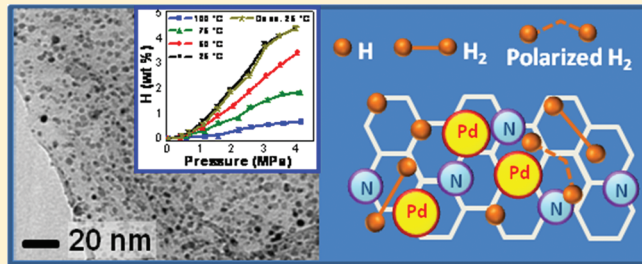
## Effect of Nitrogen Doping on Hydrogen Storage Capacity of Palladium Decorated Graphene

Vinayan Bhagavathi Parambhath, Rupali Nagar, and S. Ramaprabhu\*

Alternative Energy, Nanotechnology Laboratory (AENL), Nano Functional Materials Technology Centre (NFMTC), Department of Physics, Indian Institute of Technology Madras, Chennai, Tamil Nadu 600036, India

Supporting Information

**ABSTRACT:** A high hydrogen storage capacity for palladium decorated nitrogen-doped hydrogen exfoliated graphene nanocomposite is demonstrated under moderate temperature and pressure conditions. The nitrogen doping of hydrogen exfoliated graphene is done by nitrogen plasma treatment, and palladium nanoparticles are decorated over nitrogen-doped graphene by a modified polyol reduction technique. An increase of 66% is achieved by nitrogen doping in the hydrogen uptake capacity of hydrogen exfoliated graphene at room temperature and 2 MPa pressure. A further enhancement by 124% is attained in the hydrogen uptake capacity by palladium nanoparticle (Pd NP) decoration over nitrogen-doped graphene. The high dispersion of Pd NP over nitrogen-doped graphene sheets and strengthened interaction between the nitrogen-doped graphene sheets and Pd NP catalyze the dissociation of hydrogen molecules and subsequent migration of hydrogen atoms on the doped graphene sheets. The results of a systematic study on graphene, nitrogen-doped graphene, and palladium decorated nitrogen-doped graphene nanocomposites are discussed. A nexus between the catalyst support and catalyst particles is believed to yield the high hydrogen uptake capacities obtained.



### INTRODUCTION

In today's world, especially in the developing countries, the rising living standards have led to a sharp increase in the demand of fuels that mainly originate from the nonrenewable fossil fuels. According to a recent survey, the world energy demand rose by 5.5% in 2010 as compared to a 1.1% decrease in 2009.<sup>1</sup> With the evident changes in climate patterns all over the world, there is a growing awareness and willingness to switch over to green sources of energy. Sustainable energy production, storage, and consumption are major challenges that our world currently faces.<sup>2</sup> In this search for noncontaminating and renewable sources of energy, the fields of hydrogen energy and fuel cell technology have shown great promise.<sup>3–5</sup> In case of hydrogen energy, however, the storage of hydrogen has been identified as the most difficult challenge.<sup>6</sup> For practical applications, hydrogen storage demands high gravimetric and volumetric densities, fast reaction kinetics, a low H<sub>2</sub> sorption temperature, good reversibility, and low cost. Physical storage of hydrogen by liquefaction or pressurization requires high energy input while safety risks are also involved. Chemically stored hydrogen in materials is a safe and efficient means of storing hydrogen. The US Department of Energy has set a target of 6.5 wt % of stored hydrogen with a volume density of 62 kg/m<sup>3</sup> of H<sub>2</sub> at ambient temperature for mobile automotive applications.<sup>7</sup>

To achieve the gravimetric hydrogen storage target, lightweight materials having large surface areas emerge as a natural choice. Therefore, numerous reports can be found on carbon-

based materials which have been tested for energy-related applications and, in particular, hydrogen storage properties.<sup>2,6,8–11</sup> The carbon materials (in their pristine or modified forms) that have been focused in the past are activated carbon,<sup>9,12,13</sup> carbon nanofibers,<sup>14,15</sup> carbon nanotubes (CNTs),<sup>16,17</sup> and graphene.<sup>18,19</sup> Hydrogen can be stored in materials by sorption of either molecular hydrogen or atomic hydrogen. Owing to the low hydrogen storage capacity ( $\leq 1$  wt %) of pure carbon-based materials at ambient temperatures and moderate pressures, it has been realized that these cannot be used for practical energy storage systems.<sup>11,20</sup> Their chemical modification by functional groups or metal or metal oxide nanoparticles (NPs) is more promising and, in fact, necessary. Recently, it was reported that hydrogen storage at room temperature can be improved by a phenomenon known as *spillover effect* initiated by metal NPs decorated over the adsorbate surface.<sup>18,21–25</sup> Hydrogen spillover is defined as the dissociative chemisorption of hydrogen molecule on metal nanoparticles in the form of atomic hydrogen and subsequent migration of these hydrogen atoms onto adjacent surfaces of the adsorbate via surface diffusion. The contact between the metal NPs and supporting adsorbate material plays a vital role in spillover mechanism.<sup>26,27</sup> However, poor reversibility and the issue of structural stability in transition metal dispersions have

Received: October 24, 2011

Revised: May 1, 2012

Published: May 1, 2012

been major hurdles as the metal atoms tend to aggregate easily because of the strong metal cohesion forces. In this regard, judiciously chosen support materials can not only help in stabilizing the metal nanoparticles but also participate in the gas adsorption process. Recently, graphene has been reported as a promising candidate for hydrogen storage due to its light weight, stability, porosity, and large surface area properties, and incorporation of transition metals can enhance its hydrogen storage capacity.<sup>19</sup>

Doping or chemical modification of the carbon materials can also significantly affect the hydrogen adsorption and desorption process.<sup>28</sup> Theoretical as well as experimental studies have indicated that substitutional doping of carbon materials can be used to tailor their physical and/or chemical properties.<sup>9,10,29</sup> In particular, plenty of reports on nitrogen or boron doping of carbon-based nanomaterials have emerged recently.<sup>10,28–32</sup> It has been reported that nitrogen doping results in an increase in the conductivity as the nitrogen atoms contribute additional electron density in the parent matrix.<sup>33,34</sup> Nitrogen doping has also been found to result in an enhanced surface chemical activity in terms of polarity and basicity.<sup>35</sup> Recently it has been shown that dissociation of hydrogen can be done using electric field also in addition to the catalytic dopants.<sup>36,37</sup>

In an effort to investigate the role of nitrogen doping on graphene for hydrogen storage applications, we here report the results of a systematic study carried out on graphene, nitrogen-doped graphene, and nitrogen-doped graphene decorated with Pd nanoparticles. The nitrogen doping was carried out using nitrogen plasma treatment of graphene sheets initially prepared by hydrogen induced exfoliation.<sup>38</sup> The decoration of Pd nanoparticles on nitrogen-doped graphene was done by a modified polyol method.<sup>19</sup> A 20 loading of metal nanoparticles was intended. For reference, a mechanical mixture of Pd nanoparticle and graphene was also synthesized and studied. All the high pressure hydrogen adsorption studies reported here were carried out using Sieverts' apparatus in the temperature range from 25 to 100 °C and 0.1–4 MPa hydrogen pressure.

## ■ EXPERIMENTAL METHODS

**Synthesis of Materials.** Graphene was prepared by hydrogen exfoliation of graphite oxide (GO) which was initially prepared by Hummer's method.<sup>39</sup> The details of synthesizing hydrogen exfoliated graphene (HEG) have been published elsewhere.<sup>38</sup> The nitrogen doping of graphene (N-HEG) was carried out using nitrogen plasma treatment of HEG in a planar RF magnetron sputtering system equipped with a high-frequency generator working at a frequency of 13.56 MHz. About 300 mg of HEG was taken in a Petri dish and introduced into the plasma chamber. The chamber pressure and plasma power were maintained at 0.1 mbar and 130 W, respectively, for 30 min. The modified polyol reduction method was used to decorate palladium nanoparticles over N-HEG support. About 300 mg of N-HEG was dispersed in 300 mL of a mixture of ethylene glycol (EG) and deionized (DI) water by ultrasonication for 1 h and followed by stirring for 12 h. Further, the required amount of 1% aqueous solution of  $\text{PdCl}_2$  (6 mg of Pd/mL) was added to the solution dropwise under mechanically stirred conditions for 24 h. The pH of the entire solution was adjusted to 11 by adding NaOH (2.5 M), and the solution was refluxed at 110 °C for 7 h to ensure complete reduction of Pd. The water-to-EG ratio was controlled 1:3 throughout the reaction. In this reaction, ethylene glycol acts as a reducing, stabilizing, and dispersing agent. Finally, the suspension was filtered and the solid washed with DI water repeatedly until neutral and dried in vacuum oven at 50 °C. The sample was labeled as Pd-N-HEG. For comparison, Pd NPs prepared by the modified polyol method and HEG were mixed mechanically in a mortar and pestle for

homogeneity. The sample was labeled as Pd-HEG. The amount of palladium loading was maintained to be 20 for Pd-N-HEG and Pd-HEG specimens.

**Characterization Techniques.** The vibrational characteristics of the samples were analyzed via Raman spectroscopy using 532 nm laser (Witec Alpha 300) as the excitation source in the range from 1000 to 2000  $\text{cm}^{-1}$ . The X-ray diffraction (XRD) measurements were performed with a PANalytical X'Pert Pro X-ray diffractometer with nickel-filtered Cu K $\alpha$  radiation as the X-ray source. The pattern was recorded in the  $2\theta$  range of 5°–90° with a step size of 0.016°. The morphology of the samples was characterized by field emission scanning electron microscope (FESEM, FEI QUANTA 3D) and transmission electron microscope (TEM, Tecnai G<sup>2</sup> 20 S-TWIN, 200 keV). The samples for TEM were prepared by dispersing the specimens in ethanol and drop-casted over holey carbon-coated copper grid (200 mesh). The samples were dried overnight in ambient atmosphere. X-ray photoelectron spectroscopy (XPS, Omicron Nanotechnology) was used to determine the nitrogen content and the type of nitrogen bonding in nitrogen-doped specimen along with presence of other surface functional groups.

**High-Pressure Hydrogen Adsorption Studies.** Hydrogen adsorption studies were carried out for the HEG, N-HEG, Pd-HEG, and Pd-N-HEG nanocomposites in the pressure range 0.1–4 MPa and in the temperature range 25–100 °C using a high-pressure Sieverts' apparatus. The schematic representation of the setup has been discussed elsewhere.<sup>19</sup> The unit has been calibrated with high-purity hydrogen (99.99%) at various initial pressures. At various pressures and temperatures, the volume of gas contained in the empty sample cell was precisely measured. At high pressures, the ideal gas law was corrected using van der Waals equation for the volume of gas molecules and molecular interactions. A number of empty tests were performed, which confirmed that the system was leak-free. Each time, over 250 mg of sample was loaded in the sample cell. The samples were activated by vacuum heat treatment before exposing to hydrogen to remove the impurities such as the adsorbed water and oxide layers. In each activation process, the sample was evacuated to a vacuum of  $10^{-6}$  Torr and heated at 300 °C for 2 h. It was then cooled to 100 °C, and hydrogen was allowed to interact with the sample. The sample was subsequently cooled to 75 °C, 50 °C, and room temperature. The pressure–composition relationships were obtained by calculating the hydrogen storage capacity in wt % from the pressure drop during the hydrogen adsorption at constant temperature. After each cycle, the sample was degassed for 3 h at 200 °C under a vacuum of  $10^{-6}$  Torr. During the experiment the room temperature was maintained at 25 ± 1 °C.

## ■ RESULTS AND DISCUSSION

**Vibrational, Structural, and Morphological Studies.** Figure 1 shows the Raman spectra of (a) HEG, (b) N-HEG, and (c) Pd-N-HEG specimens. The corresponding spectra of graphite and Pd-HEG have been shown in the Supporting Information as Figure S1. In case of graphite, a very sharp peak appears at 1577  $\text{cm}^{-1}$  corresponding to the optically allowed E<sub>2g</sub> phonons at the Brillouin zone center (see Figure S1).<sup>40</sup> This is the G-band, which arises from the stretching of the C–C bond in graphitic materials, and is common to all sp<sup>2</sup> carbon systems.<sup>41</sup> A very small feature at 1350  $\text{cm}^{-1}$  is also detected which corresponds to the defect band in graphite, often termed as the D-band, that arises due to the disorder in the sp<sup>2</sup> hybridization. In case of HEG, the position of G- and D-bands is observed respectively at 1581 and 1352  $\text{cm}^{-1}$ . The intensity of D-band exceeds that of the G-band, suggesting that the structure comprises of numerous defects as a result of exfoliation. It is well-known that the position of the G-band is very sensitive to the strain present in the specimen in all sp<sup>2</sup> systems. The observed blue-shift in case of the G-band of HEG is indicative of the compressive stresses that may have

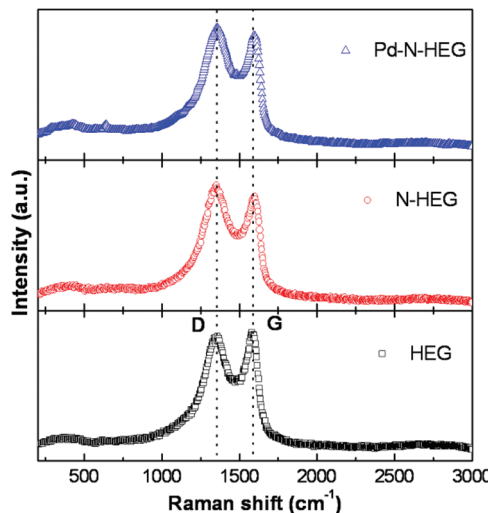


**Figure 1.** Raman spectra of (a) HEG, (b) N-HEG, and (c) Pd-N-HEG samples in the range 200–3000 cm<sup>-1</sup> depicting the G- and D-bands around 1580 and 1351 cm<sup>-1</sup>, respectively.

developed postexfoliation, leading to a higher degree of wrinkled morphology of the graphene sheets. Thermodynamically, the existence of a two-dimensional flat sheet of graphene is not favorable. As a result, the sheets fold in their planes or at the edges, creating a wrinkled morphology making the structure thermodynamically stable. In case of N-HEG, the G-band is observed to shift further to a position of 1592 cm<sup>-1</sup>, suggesting the incorporation of nitrogen atoms in the carbon network,<sup>42</sup> while the position of D-band is observed at 1352 cm<sup>-1</sup>. The positions of G- and D-bands in case of Pd-N-HEG are observed at 1597 and 1353 cm<sup>-1</sup>. In addition, a small shoulder appears in case of Pd-N-HEG at the higher wavenumbers along with the G-band. This is known as the D\* band.<sup>43</sup> The origin of this band is attributed to the interaction of localized vibration modes of impurities (or dopants) with the extended phonon modes of graphene responsible for the G-band.<sup>44</sup> After Pd nanoparticle attachment the G-band is observed to shift further toward higher wavenumbers. The ratio of the intensity of the D- and G-band expressed as  $I_D/I_G$  is taken as a measure of the degree of defects present in the specimen. Comparing the ratios of  $I_D/I_G$  across HEG, N-HEG, and Pd-N-HEG, we find that the ratio changes from 0.98 for HEG to 1.01 for N-HEG and to 1.05 for Pd-N-HEG, indicating that the defect states increase as a result of N-doping and Pd NP decoration.

Figure 2 shows the XRD diffractograms of the as-synthesized (a) HEG, (b) N-HEG, and (c) Pd-N-HEG samples. The appearance of a broad diffraction peak ranging from  $2\theta$  value of 18° to 28° in all cases corresponds to the (002) plane of graphitic carbon and indicates the presence of graphene sheets in the specimen. This broadening of the diffraction peak suggests the lack of long-range order and is a signature of graphene-based specimens. The interlayer spacing (*d*-spacing) is observed to increase by 8–9% as compared to the 0.34 nm *d*-spacing along the *c*-axis of the starting graphite powder. The presence of C(101) peak can also be seen. The XRD diffractogram of N-HEG is similar to that of HEG. In the case of Pd-HEG (see Figure S2 of Supporting Information) and Pd-N-HEG (Figure 1b) samples, the fingerprint peaks of palladium corresponding to the (111), (200), (220), (311), and (222) plane reflections are observed, confirming the incorporation of Pd particles within the specimens. The Pd crystallite

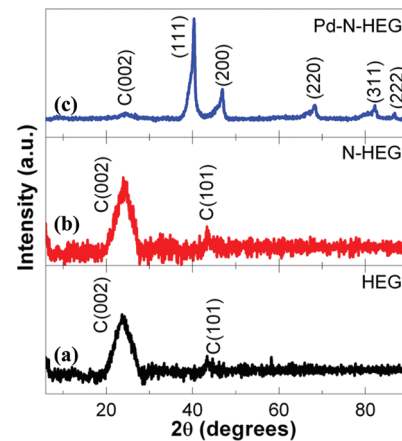


**Figure 2.** X-ray diffractograms of (a) HEG, (b) N-HEG, and (c) Pd-N-HEG. The Pd fingerprint peaks and carbon peaks have been indicated against the respective peaks.

size determined by Scherrer's formula is observed to be about 8.2 nm for Pd-HEG and 5.8 nm for Pd-N-HEG.

Figure 3 depicts the SEM micrographs of (a) N-HEG and (b) Pd-N-HEG samples. Several graphene layers and folds in

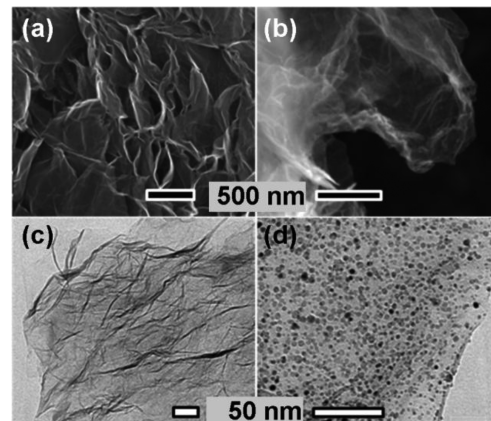


**Figure 3.** (a) Scanning electron micrographs of (a) N-HEG and (b) Pd-N-HEG depicting the folds in graphene layers. Transmission electron micrographs of (c) N-HEG and (d) Pd-N-HEG. A uniform dispersion of Pd NPs on N-HEG support is clearly visible.

their planes are visible. Figures 3c and 3d depict the TEM micrographs of N-HEG and Pd-N-HEG, respectively. A uniform dispersion of Pd NPs can be seen from Figure 3d. The TEM micrographs for HEG and Pd-HEG have been shown in the Supporting Information as Figure S3. The degree of exfoliation is seen to be higher in case of HEG as compared to Pd-HEG. This may be due to the process of mechanical mixing of graphene with Pd NPs where there is probability of sheets being restacked to some extent. The TEM micrograph of Pd-HEG (Figure S3) shows large sized (~50 nm) agglomerates of Pd particles supported on the graphene sheets. A comparison between Figure S3 and Figure 3b reveals that dispersion of NPs is excellent in the latter case. The particle size in case of Pd-N-HEG from TEM micrographs has been estimated to be 3.1 ± 0.6 nm. The small particle size of Pd NPs in Pd-N-HEG may be due to the incorporation which affects the nucleation of Pd nanoparticles.<sup>45</sup> This is attributed to the fact that the N-doping creates a defective topology in the graphene network of HEG,

which then act as nucleation sites for the Pd particle to get attached during the modified polyol synthesis method.

Figures 4a–d show the core level XPS spectra of C 1s, N 1s, Pd 3d, and O 1s orbitals of Pd-N-HEG sample, respectively.

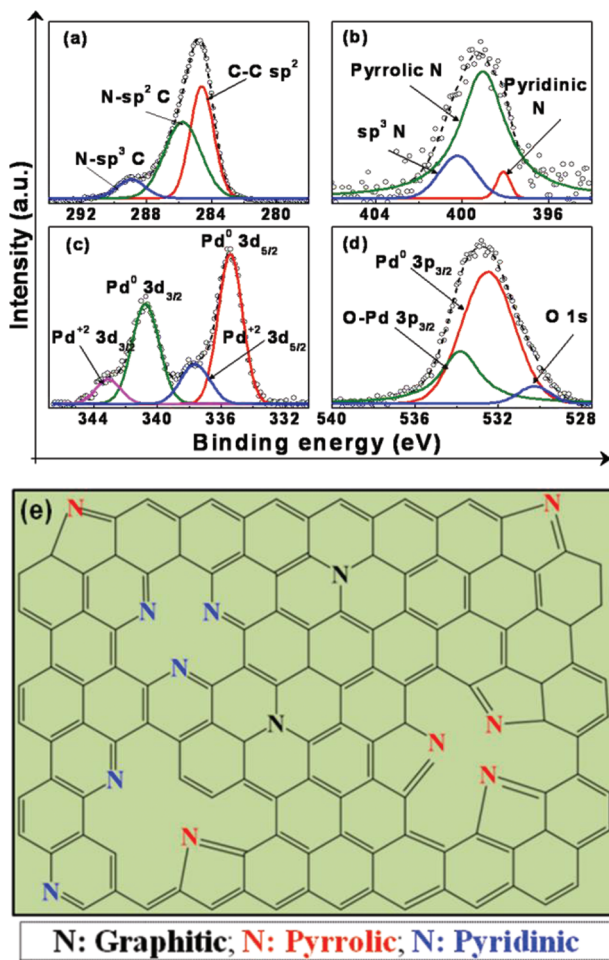


**Figure 4.** High-resolution X-ray photoelectron spectra of (a) carbon, (b) nitrogen, (c) palladium, and (d) oxygen elements of Pd-N-HEG sample. (e) Schematic of nitrogen-doped graphene depicting the nature of bonding of nitrogen atoms in the graphene network.

From Figure 4a, the presence of  $sp^2$  C 1s peak is observed to be at 284.25 eV. The presence of carbon–nitrogen bonds is also detected at 285.78 and 288.94 eV which are attributed to  $sp^2$  C–N and  $sp^3$  C–N bonds, respectively.<sup>46,47</sup> From the nitrogen high-resolution XPS scan shown in Figure 4b, it is observed that three different types of nitrogen are present in the Pd-N-HEG system, namely, pyridinic nitrogen (398.1 eV), pyrrolic nitrogen (399.04 eV), and  $sp^3$  C–N bond (400.21 eV). The schematic in Figure 4e depicts the incorporation of these different types of nitrogen within the graphene network. From XPS results, the nitrogen content is estimated to be about 7 at. %. The pyridinic and pyrrolic nitrogen atoms donate  $\pi$ -electron density in carbon network of graphene lattice and contribute to the  $sp^2$  character of the graphene network. From XPS analysis it is observed that the content of pyrrolic nitrogen is more in the Pd-N-HEG sample. The Pd<sup>0</sup> 3d<sub>5/2</sub> and 3d<sub>3/2</sub> doublets are observed at 335.43 and 340.76 eV, respectively, as shown in Figure 4c. Palladium is also detected in the +2 oxidation state (doublet pair at 337.28 and 342.74 eV), and this higher oxidation state of Pd may be due to the formation of Pd–O

bond or Pd–N bond.<sup>48</sup> The high-resolution scan from 528 to 544 eV reveals the presence of Pd 3p<sub>3/2</sub>, Pd–O, and O 1s peaks in that order of their percentage contribution as shown in Figure 4d. The concentration of Pd was estimated from XPS Pd 3d peaks and was found to be 21 wt %. This is in agreement with the energy dispersive X-ray analysis (shown as Figure S4 in the Supporting Information), which estimates the Pd concentration to be 20 wt %.

**Hydrogen Storage Capacity of Pd-N-HEG.** Figure 5 shows the pressure–composition isotherms of (a) N-HEG and

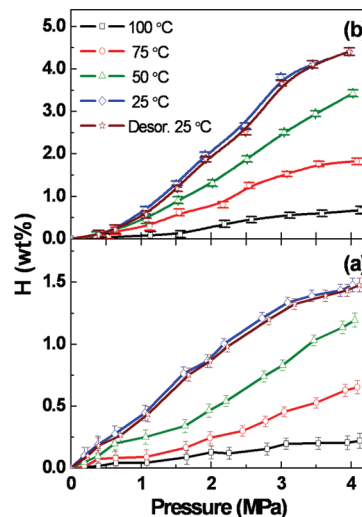


**Figure 5.** Pressure–composition isotherms of (a) N-HEG and (b) Pd-N-HEG in the temperature range 25–100 °C and 0.1–4 MPa pressure.

(b) Pd-N-HEG acquired in the temperature range of 25–100 °C and pressure range of 0.1–4 MPa, respectively. The maximum capacity of 4.4 wt % has been achieved at 25 °C and 4 MPa pressure of hydrogen. The pressure–composition isotherms for HEG and Pd-HEG specimens have been shown in the Supporting Information as Figure S5. It is observed that with increasing temperatures the hydrogen adsorption capacity at different pressures decreases for all specimens. This is because gas molecules possess higher kinetic energy and can easily cross the activation energy barrier required for desorbing from the adsorbed sites. Comparing the hydrogen uptake capacity at 25 °C and 2 MPa, it is observed that the uptake capacity increases from 0.53% for HEG to 0.63% for Pd-HEG and 0.88% for N-HEG. Therefore, nitrogen doping is more effective in increasing the adsorption of hydrogen than the mechanically mixed Pd-HEG nanocomposite. It should be, however, borne that the Pd-HEG composite comprises of large sized Pd particle agglomerates (see Figure S3). In case of the Pd-N-HEG specimen, where a more uniform dispersion has been achieved, the hydrogen uptake attains a value of 1.97% at 25 °C and 2 MPa pressure. The present hydrogen uptake is very high as compared to previously reported Pd decorated carbon nanotubes and carbon supports.<sup>49–51</sup> In our previous study, we have studied the role of oxygen-based functional groups in Pd decorated graphene for hydrogen storage applications, which shows the hydrogen uptake capacity of 3 wt % at 4 MPa hydrogen pressure at 25 °C temperature.<sup>19</sup> This amounts to about 47% increase in the hydrogen uptake capacity (at 4 MPa, 25 °C) of Pd-N-HEG as compared to Pd NP decorated functionalized-graphene and strengthens the candi-

dature of nitrogen-doped graphene as a support for dispersing NPs for storage media applications. The weight percentage of hydrogen stored by HEG, N-HEG, Pd-HEG mixture, Pd NPs on functionalized graphene, and Pd NPs on nitrogen-doped graphene have been tabulated in Table S1 of the Supporting Information.

The shape of the pressure–composition isotherms can suggest the underlying mechanism for gas adsorption. The nature of adsorption isotherms in case of HEG and Pd-HEG is of type I, implying that mostly the adsorption of hydrogen gas occurs in the micropores of the specimens. This can be attributed to the presence of pores in the graphene sheets and also indicates the inefficient hydrogen adsorption by the Pd particle agglomerates. The shape of the isotherms in case of N-HEG and Pd-N-HEG resemble type II adsorption isotherms that signify adsorption in macroporous adsorbates with strong interaction between adsorbate and adsorbents. The interaction between the hydrogen gas and nitrogen-doped graphene is stronger than pristine graphene and is therefore reflected from the isotherm study and corroborates the findings of other researchers, which is now briefly discussed. We believe that the support plays two important roles. It independently affects the gas adsorption process as compared to pristine graphene and also stabilizes the Pd nanoparticles on the support. We first look at the interaction of hydrogen molecules in the presence of nitrogen doped graphene.

**Role of Nitrogen Doping on Graphene Supports.** It is well-known that the process of physisorption is based on the van der Waals interaction between the gas molecules and the surface of the adsorbate. Therefore, the interaction between the adsorbate and the adsorbent can be strengthened if the charge distribution on the adsorbate's surface can be tailored. In this regard, the polarizability of the adsorbate plays a crucial role. Since nitrogen has one extra valence electron as compared to carbon, doping with nitrogen enhances the  $\pi$ -electron density in carbon network of graphene locally at the heteroatom site and its carbon neighbors. From XPS analysis it was observed that the pyrrolic nitrogen is present more than pyridinic nitrogen. The pyrrolic nitrogen atoms are known to donate two  $\pi$ -electrons as compared to one  $\pi$ -electron from pyridinic nitrogen. This added electron density at the doped sites induces an asymmetry in the local electronic density, thereby increasing C–H interaction as compared to pristine graphene by increasing the polarizability of gas molecules. The enhancement observed in the hydrogen uptake capacity of pristine graphene by utilizing nitrogen doping lends support to this hypothesis (see Table S1, Supporting Information). In a study by Sankaran and Viswanathan on heteroatom substituted carbon nanotubes, the authors show that (i) the heteroatom like nitrogen cause a decrease in the hydrogen dissociation energy in the geometrically and chemically substituted nanotubes and (ii) upon hydrogenation the formation of N–H bond is favorable as compared to C–H bond.<sup>52</sup> The bond length of the hydrogen molecule is elongated in heteroatom substituted nanotubes compared to that of pure carbon nanotubes, indicating that there is a considerable amount of activation of hydrogen molecule in heteroatom containing carbon nanotubes.<sup>52</sup> This result is in agreement with the *ab initio* calculations of Zhang and Cho on pristine and nitrogen-doped carbon nanotubes which show that nitrogen doping alters the catalytic effects of the carbon nanotube for hydrogen dissociative adsorption.<sup>53</sup> Taking the contribution of C, N, and H atoms toward the highest occupied molecular orbital into account, Sankaran and

Viswanathan have shown that the p orbital of the heteroatom and the 1s orbital of H participate in bonding, establishing the formation of N–H bond in the process. Furthermore, the hydrogen molecule activated at the heteroatom site subsequently migrates to the carbon sites.<sup>52</sup> Similar effects can be expected in case of nitrogen-doped graphene where activation of hydrogen molecule may occur near the nitrogen atom sites. The schematic in Figure 6 (top panel) shows the elongation of

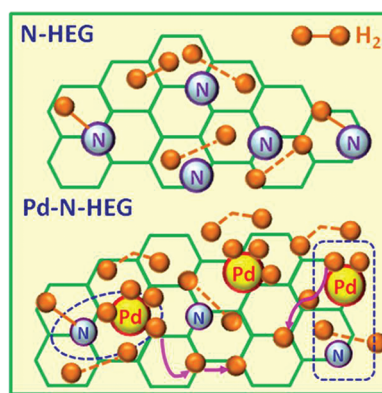


**Figure 6.** Schematic shows the possible formation of bonds upon hydrogenation of N-HEG (top panel) and Pd-N-HEG (bottom panel). Elongation of bonds is depicted by dashed lines. On approaching Pd NPs, the H<sub>2</sub> molecules may get polarized as shown by bent bonds or dissociate into H atoms. Once a Pd NP is saturated, the H atoms may then diffuse on the carbon support as shown by pink arrows.

H–H bond (by dashed lines) and the possibility of formation of N–H bond upon the hydrogenation of N-HEG specimen. Next, the role of nitrogen-doped carbon support and metal NPs is discussed in detail.

**Role of Nitrogen Doping on Transition Metal Nanoparticles.** The decoration of carbon support by transition metals can also be independently used to enhance the hydrogen storage of the specimens. Transition metals eliminate the hydrogen dissociation barrier altogether.<sup>22</sup> But some transition metals like Ti bind strongly with hydrogen atoms and impede their migration on the carbon support. As a result, once the metal nanoparticle is saturated with hydrogen atoms, it cannot further uptake the hydrogen and thus becomes inactive. Therefore, not only the catalyst NPs should bind hydrogen atoms but should also allow the dissociated hydrogen atoms to migrate away on the support after saturation. In this context, transition metals like Pd are more promising as they do not bind with H atoms strongly and can promote their migration to the carbon support underneath. Both experimental and theoretical studies have been reported in relation to the transition metals–graphene composite for hydrogen storage applications. Srinivas et al. have reported that graphene nanosheets can store hydrogen better than that of carbon nanotubes and graphite.<sup>54</sup> In yet another study, few-layered graphene has been shown to achieve a hydrogen storage capacity of 3.1 wt % at high pressures and temperature of 300 K.<sup>55</sup> The first-principle studies by Banerjee et al. show that transition metal atoms on Mg surface influence the hydrogen dissociation or hydrogen diffusion barriers.<sup>56,57</sup> Another theoretical report shows that calcium-decorated zigzag graphene nanoribbon can reach the gravimetric capacity of ~5 wt % hydrogen.<sup>58</sup> Ao and Peeters have shown that

theoretically a graphene layer with aluminum adsorbed on both sides can store hydrogen up to 13.79 wt % with average adsorption energy  $-0.193$  eV per H<sub>2</sub>.<sup>59</sup> Ao and Peeters have also reported the catalytic effects of nitrogen doping and electric field on the dissociative adsorption of hydrogen on graphene sheets by density functional theory.<sup>36,37</sup> Recently, we investigated the hydrogen storage capacity on Pd NPs decorated functionalized graphene, where after dissociation the surface oxygen based functional groups act as bridges for H atoms to migrate from the Pd NPs onto the graphene sheets. As reported in Table S1, a 1.76 wt % of hydrogen could be stored at 2 MPa and 25 °C.<sup>19</sup> The process of acid functionalization was followed to attach oxygen functional groups on graphene, which may lead to restacking of graphene sheets to some extent and thus reduce its surface area. The attached functional groups serve as nucleation sites of Pd NPs. These Pd nanoparticles attached on functionalized graphene are only weakly adhered to the carbon support, and the possibility of their detachment and subsequent agglomeration exists. As discussed earlier, doping of graphene sheets with acceptor or donor type of heteroatom provides an avenue for tailoring the electronic density of the carbon network that can be suitably exploited for various applications without adversely affecting properties like high surface area. In particular, it can be used to stabilize the metal nanoparticles decorated on the carbon support. Nitrogen doping of graphene can help in enhancing the metal binding to the defected sites on the adsorbant, thereby lowering the possibility of metal–metal cohesion. Recently, Wu et al. have theoretically investigated the role of Pt NP decorated boron-doped graphene for hydrogen storage.<sup>30</sup> Their density functional theory calculations show that in the case of pristine graphene the platinum clusters have a tendency to detach from the graphene sheets upon hydrogenation. However, in boron-doped graphene, the increased interaction between the support and metal particles minimizes the detachment of Pt NPs from the support and also favors chemisorption of more number of H atoms. Corral et al. have recently studied the changes in the bonding of Pd–graphene upon hydrogenation by density functional theory (DFT).<sup>60</sup> The authors have shown that a Pd atom prefers to adsorb on the C–C bridge site as compared to any other available site on the hexagonal cell of graphene. Their DFT results show that the C–C bonds near the Pd adsorption site are weakened after Pd decoration process due to the formation of Pd–C bonds. On adsorption of hydrogen new Pd–H bonds were found to form at the expense of weakening of Pd–C and C–C bonds. No new formation of C–H bonds was found.<sup>60</sup> For further details on the interaction between hydrogen and Pd–graphene the reader is referred to the section on “interaction of hydrogen with Pd adsorbed on graphene” provided in the Supporting Information. Interestingly, even after hydrogenation a Pd–C bond still existed establishing that Pd decoration stays on graphene and that Pd NPs act as “bypass” for hydrogen to transfer to the carbon support. The attachment of Pd NPs on carbon support usually occurs by a small donation of electrons from Pd 4d orbitals to C 2s orbitals and then a back-donation from C 2p to Pd 5s orbitals.<sup>60</sup> In the present work where N-HEG has been used as the support material, the carbon atoms in the vicinity of nitrogen atoms develop an increased  $\pi$ -electron density which makes the back-donation to 5s orbitals of Pd easier and strengthens the Pd–C interaction. Horinouchi et al. have reported that back-donation interaction usually increases when the oxidation state of

palladium decreases.<sup>61</sup> The zerovalent Pd atoms present in Pd-N-HEG as confirmed from XPS analysis, therefore, may facilitate the electron back-donation process. The nitrogen atoms also serve as the sites where Pd NP nucleation and growth occurs and results in a uniform dispersion of Pd NPs. The Pd transition metal NPs aid in reducing the energy required for hydrogen molecule dissociation. After the dissociation of hydrogen molecules, once Pd nanoparticle is saturated with hydrogen atoms, they may migrate away from the nanoparticle onto the support and subsequently diffuse on the adsorbate surface. The strong binding between Pd NPs and graphene surface via nitrogen atoms prevents the detachment of Pd nanoparticles and allows the migration of hydrogen atoms to the adsorbate surface. For illustration, the process has been depicted as a schematic in Figure 6 (bottom panel). The enhancement in the hydrogen uptake capacity of Pd-N-HEG sample, as compared to the hydrogen storage capacity of individual components within the nanocomposite such as N-HEG and Pd NPs, is estimated as follows:<sup>19</sup>

$$\begin{aligned} \text{wt \%}_{\text{enhancement}} &= \text{wt \%}_{\text{Pd-N-HEG}} - (100 - q) \times \text{wt \%}_{\text{N-HEG}} \\ &\quad - q \times \text{wt \%}_{\text{PdNP}} \end{aligned} \quad (1)$$

Here, wt % indicates the weight percentage of stored hydrogen and the corresponding subscript denotes the specimen under investigation, and  $q$  denotes the weight percentage of Pd in Pd-N-HEG specimen. On substituting the hydrogen uptake values of respective samples at 25 °C and 2 MPa pressure, the enhancement in the hydrogen uptake capacity is found to be  $\text{wt \%}_{\text{enhancement}} = 1.97 - (0.8) \times 0.88 - (0.20) \times 0.72 \approx 1.12$ .

Therefore, about 1.12 wt % of enhancement in hydrogen uptake capacity was observed in Pd-N-HEG under moderate temperature and pressure conditions because of high dispersion and strong bonding of Pd NPs over nitrogen-doped graphene. The charge transfer between the modified electronic structure of graphene after nitrogen doping and the TM d orbitals plays a crucial role for uniform metal dispersion and strengthened interaction and successive enhancement in the hydrogen adsorption.<sup>62</sup> Therefore, a nexus between the catalyst support and catalyst particles is believed to yield the high hydrogen uptake capacities observed in the present work. The detailed studies on HEG, N-HEG, and Pd-N-HEG are an experimental proof for numerous theoretical studies such that the doping effects on carbon support materials and the uniform dispersion, optimum particle size, and strong binding of TM NPs over these doped carbon supports. All these are crucial factors which together can enhance the hydrogen storage capacity.

## CONCLUSION

The hydrogen storage study of nitrogen-doped graphene and graphene demonstrates the enhanced interaction of hydrogen molecules with the nitrogen-doped graphene as compared to pure graphene. The Pd decoration over the nitrogen-doped graphene can be used to enhance the hydrogen uptake capacity of graphene by almost 272% at ambient temperature and under moderate pressure of 2 MPa. The highly dispersed and strongly adhered Pd nanoparticles over nitrogen-doped graphene reduce the dissociation barrier for hydrogen molecules and subsequent migration of hydrogen atoms to the support. The charge transfer between the modified electronic structure of graphene after nitrogen doping and the transition metal d orbitals leads to the excellent metal dispersion and strong binding of the

catalyst nanoparticles that subsequently give rise to enhanced hydrogen storage capacity.

## ■ ASSOCIATED CONTENT

### § Supporting Information

Raman spectra of graphite and Pd-HEG, XRD diffractogram of Pd-HEG, TEM micrographs of HEG and Pd-HEG, EDX spectrum of Pd-N-HEG, pressure–composition isotherms of HEG and Pd-HEG, table with the weight percentage of hydrogen stored by different specimens at 25 °C and 2, 4 MPa, and the detailed description of the interaction of hydrogen on graphene and nitrogen-doped graphene with Pd. This material is available free of charge via the Internet at <http://pubs.acs.org>.

## ■ AUTHOR INFORMATION

### Corresponding Author

\*Ph +91-44-22574862, Fax +91-44-22570509/22574852, e-mail ramp@iitm.ac.in.

### Notes

The authors declare no competing financial interest.

## ■ ACKNOWLEDGMENTS

The authors gratefully acknowledge IIT Madras, MNRE, and DST, India, for supporting this work.

## ■ REFERENCES

- (1) Enerdata, Global Energy Statistical Yearbook, 2011.
- (2) Pumera, M. Graphene-based nanomaterials for energy storage. *Energy Environ. Sci.* **2011**, *4*, 668–674.
- (3) Germain, J.; Fréchet, J. M. J.; Svec, F. Nanoporous Polymers for Hydrogen Storage. *Small* **2009**, *5*, 1098–1111.
- (4) Paul, R. K.; Ghazinejad, M.; Penchev, M.; Lin, J.; Ozkan, M.; Ozkan, C. S. Synthesis of a Pillared Graphene Nanostructure: A Counterpart of Three-Dimensional Carbon Architectures. *Small* **2010**, *6*, 2309–2313.
- (5) Wildgoose, G. G.; Banks, C. E.; Compton, R. G. Metal Nanoparticles and Related Materials Supported on Carbon Nanotubes: Methods and Applications. *Small* **2006**, *2*, 182–193.
- (6) Jena, P. Materials for Hydrogen Storage: Past, Present, and Future. *J. Phys. Chem. Lett.* **2011**, *2*, 206–211.
- (7) Energy, D. o. A Multiyear Plan for the Hydrogen R&D Program, Aug 1999.
- (8) Huang, X.; Yin, Z.; Wu, S.; Qi, X.; He, Q.; Zhang, Q.; Yan, Q.; Boey, F.; Zhang, H. Graphene-Based Materials: Synthesis, Characterization, Properties, and Applications. *Small* **2011**, *7*, 1876–1902.
- (9) Ströbel, R.; Garche, J.; Moseley, P. T.; Jörissen, L.; Wolf, G. Hydrogen storage by carbon materials. *J. Power Sources* **2006**, *159*, 781–801.
- (10) Jiang, J.; Gao, Q.; Zheng, Z.; Xia, K.; Hu, J. Enhanced room temperature hydrogen storage capacity of hollow nitrogen-containing carbon spheres. *Int. J. Hydrogen Energy* **2010**, *35*, 210–216.
- (11) Kowalczyk, P.; Holyst, R.; Terrones, M.; Terrones, H. Hydrogen storage in nanoporous carbon materials: myth and facts. *Phys. Chem. Chem. Phys.* **2007**, *9*, 1786–1792.
- (12) Bénard, P.; Chahine, R. Determination of the Adsorption Isotherms of Hydrogen on Activated Carbons above the Critical Temperature of the Adsorbate over Wide Temperature and Pressure Ranges. *Langmuir* **2001**, *17*, 1950–1955.
- (13) Fang, B.; Kim, M.; Kim, J. H.; Yu, J.-S. Controllable Synthesis of Hierarchical Nanostructured Hollow Core/Mesopore Shell Carbon for Electrochemical Hydrogen Storage. *Langmuir* **2008**, *24*, 12068–12072.
- (14) de la Casa-Lillo, M. A.; Lamari-Darkrim, F.; Cazorla-Amorós, D.; Linares-Solano, A. Hydrogen Storage in Activated Carbons and Activated Carbon Fibers. *J. Phys. Chem. B* **2002**, *106*, 10930–10934.
- (15) Lueking, A. D.; Yang, R. T.; Rodriguez, N. M.; Baker, R. T. K. Hydrogen Storage in Graphite Nanofibers: Effect of Synthesis Catalyst and Pretreatment Conditions. *Langmuir* **2003**, *20*, 714–721.
- (16) Assfour, B.; Leoni, S.; Seifert, G.; Baburin, I. A. Packings of Carbon Nanotubes – New Materials for Hydrogen Storage. *Adv. Mater.* **2011**, *23*, 1237–1241.
- (17) Lan, A.; Mukasyan, A. Hydrogen Storage Capacity Characterization of Carbon Nanotubes by a Microgravimetric Approach. *J. Phys. Chem. B* **2005**, *109*, 16011–16016.
- (18) Wang, Y.; Guo, C. X.; Wang, X.; Guan, C.; Yang, H.; Wang, K.; Li, C. M. Hydrogen storage in a Ni-B nanoalloy-doped three-dimensional graphene material. *Energy Environ. Sci.* **2011**, *4*, 195–200.
- (19) Vinayan, B. P.; Nagar, R.; Sethupathi, K.; Ramaprabhu, S. Investigation of Spillover Mechanism in Palladium Decorated Hydrogen Exfoliated Functionalized Graphene. *J. Phys. Chem. C* **2011**, *115*, 15679–15685.
- (20) Bacsa, R.; Laurent, C.; Morishima, R.; Suzuki, H.; Le Lay, M. Hydrogen Storage in High Surface Area Carbon Nanotubes Produced by Catalytic Chemical Vapor Deposition. *J. Phys. Chem. B* **2004**, *108*, 12718–12723.
- (21) Panayotov, D. A.; Yates, J. T. Spectroscopic Detection of Hydrogen Atom Spillover from Au Nanoparticles Supported on TiO<sub>2</sub>: Use of Conduction Band Electrons. *J. Phys. Chem. C* **2007**, *111*, 2959–2964.
- (22) Adams, B. D.; Ostrom, C. K.; Chen, S.; Chen, A. High-Performance Pd-Based Hydrogen Spillover Catalysts for Hydrogen Storage. *J. Phys. Chem. C* **2010**, *114*, 19875–19882.
- (23) Lachawiec, A. J.; Qi, G.; Yang, R. T. Hydrogen Storage in Nanostructured Carbons by Spillover: Bridge-Building Enhancement. *Langmuir* **2005**, *21*, 11418–11424.
- (24) Chen, H.; Yang, R. T. Catalytic Effects of TiF<sub>3</sub> on Hydrogen Spillover on Pt/Carbon for Hydrogen Storage. *Langmuir* **2010**, *26*, 15394–15398.
- (25) Saha, D.; Deng, S. Hydrogen Adsorption on Ordered Mesoporous Carbons Doped with Pd, Pt, Ni, and Ru. *Langmuir* **2009**, *25*, 12550–12560.
- (26) Stadie, N. P.; Purewal, J. J.; Ahn, C. C.; Fultz, B. Measurements of Hydrogen Spillover in Platinum Doped Superactivated Carbon. *Langmuir* **2010**, *26*, 15481–15485.
- (27) Stuckert, N. R.; Wang, L.; Yang, R. T. Characteristics of Hydrogen Storage by Spillover on Pt-Doped Carbon and Catalyst-Bridged Metal Organic Framework. *Langmuir* **2010**, *26*, 11963–11971.
- (28) Zeng, H.; Zhao, J.; Wei, J. W.; Hu, H. F. Effect of N doping and Stone-Wales defects on the electronic properties of graphene nanoribbons. *Eur. Phys. J. B* **2011**, *79*, 335–340.
- (29) Sankaran, M.; Viswanathan, B.; Srinivasa Murthy, S. Boron substituted carbon nanotubes—How appropriate are they for hydrogen storage? *Int. J. Hydrogen Energy* **2008**, *33*, 393–403.
- (30) Wu, H.-Y.; Fan, X.; Kuo, J.-L.; Deng, W.-Q. DFT Study of Hydrogen Storage by Spillover on Graphene with Boron Substitution. *J. Phys. Chem. C* **2011**, *115*, 9241–9249.
- (31) Lin, Y.-C.; Lin, C.-Y.; Chiu, P.-W. Controllable graphene N-doping with ammonia plasma. *Appl. Phys. Lett.* **2010**, *96*, 133110–3.
- (32) Lee, D. H.; Lee, J. A.; Lee, W. J.; Kim, S. O. Flexible Field Emission of Nitrogen-Doped Carbon Nanotubes/Reduced Graphene Hybrid Films. *Small* **2011**, *7*, 95–100.
- (33) Shao, Y.; Sui, J.; Yin, G.; Gao, Y. Nitrogen-doped carbon nanostructures and their composites as catalytic materials for proton exchange membrane fuel cell. *Appl. Catal., B* **2008**, *79*, 89–99.
- (34) Panchakarla, L. S.; Subrahmanyam, K. S.; Saha, S. K.; Govindaraj, A.; Krishnamurthy, H. R.; Waghmare, U. V.; Rao, C. N. R. Synthesis, Structure, and Properties of Boron- and Nitrogen-Doped Graphene. *Adv. Mater.* **2009**, *21*, 4726–4730.
- (35) Chetty, R.; Kundu, S.; Xia, W.; Bron, M.; Schuhmann, W.; Chirila, V.; Brandl, W.; Reinecke, T.; Muhler, M. PtRu nanoparticles supported on nitrogen-doped multiwalled carbon nanotubes as catalyst for methanol electrooxidation. *Electrochim. Acta* **2009**, *54*, 4208–4215.

- (36) Ao, Z. M.; Peeters, F. M. Electric field: A catalyst for hydrogenation of graphene. *Appl. Phys. Lett.* **2010**, *96*, 253106–3.
- (37) Ao, Z. M.; Peeters, F. M. Electric Field Activated Hydrogen Dissociative Adsorption to Nitrogen-Doped Graphene. *J. Phys. Chem. C* **2010**, *114*, 14503–14509.
- (38) Kaniyoor, A.; Baby, T. T.; Ramaprabhu, S. Graphene synthesis via hydrogen induced low temperature exfoliation of graphite oxide. *J. Mater. Chem.* **2010**, *20*, 8467–8469.
- (39) Hummers, W. S.; Offeman, R. E. Preparation of Graphitic Oxide. *J. Am. Chem. Soc.* **1958**, *80*, 1339–1339.
- (40) Reich, S.; Thomsen, C. Raman spectroscopy of graphite. *Philos. Trans. R. Soc., A* **2004**, *362*, 2271–2288.
- (41) Hao, Y.; Wang, Y.; Wang, L.; Ni, Z.; Wang, Z.; Wang, R.; Koo, C. K.; Shen, Z.; Thong, J. T. L. Probing Layer Number and Stacking Order of Few-Layer Graphene by Raman Spectroscopy. *Small* **2010**, *6*, 195–200.
- (42) Shao, Y.; Zhang, S.; Engelhard, M. H.; Li, G.; Shao, G.; Wang, Y.; Liu, J.; Aksay, I. A.; Lin, Y. Nitrogen-doped graphene and its electrochemical applications. *J. Mater. Chem.* **2010**, *20*, 7491–7496.
- (43) Guo, B.; Liu, Q.; Chen, E.; Zhu, H.; Fang, L.; Gong, J. R. Controllable N-Doping of Graphene. *Nano Lett.* **2010**, *10*, 4975–4980.
- (44) Rao, C. N. R.; Sood, A. K.; Subrahmanyam, K. S.; Govindaraj, A. Graphene: The New Two-Dimensional Nanomaterial. *Angew. Chem., Int. Ed.* **2009**, *48*, 7752–7777.
- (45) Zhou, Y.; Neyerlin, K.; Olson, T. S.; Pylypenko, S.; Bult, J.; Dinh, H. N.; Gennett, T.; Shao, Z.; O’Hayre, R. Enhancement of Pt and Pt-alloy fuel cell catalyst activity and durability via nitrogen-modified carbon supports. *Energy Environ. Sci.* **2010**, *3*, 1437–1446.
- (46) Wei, D.; Liu, Y.; Wang, Y.; Zhang, H.; Huang, L.; Yu, G. Synthesis of N-Doped Graphene by Chemical Vapor Deposition and Its Electrical Properties. *Nano Lett.* **2009**, *9*, 1752–1758.
- (47) Wang, H.; Zhang, C.; Liu, Z.; Wang, L.; Han, P.; Xu, H.; Zhang, K.; Dong, S.; Yao, J.; Cui, G. Nitrogen-doped graphene nanosheets with excellent lithium storage properties. *J. Mater. Chem.* **2011**, *21*, S430–S434.
- (48) Hasik, M.; Bernasik, A.; Drelinkiewicz, A.; Kowalski, K.; Wenda, E.; Camra, J. XPS studies of nitrogen-containing conjugated polymers–palladium systems. *Surf. Sci.* **2002**, *507*–*510*, 916–921.
- (49) Zacharia, R.; Kim, K. Y.; Fazle Kibria, A. K. M.; Nahm, K. S. Enhancement of hydrogen storage capacity of carbon nanotubes via spill-over from vanadium and palladium nanoparticles. *Chem. Phys. Lett.* **2005**, *412*, 369–375.
- (50) Yoo, E.; Gao, L.; Komatsu, T.; Yagai, N.; Arai, K.; Yamazaki, T.; Matsuishi, K.; Matsumoto, T.; Nakamura, J. Atomic Hydrogen Storage in Carbon Nanotubes Promoted by Metal Catalysts. *J. Phys. Chem. B* **2004**, *108*, 18903–18907.
- (51) Campesi, R.; Cuevas, F.; Gadiou, R.; Leroy, E.; Hirscher, M.; Vix-Guterl, C.; Latroche, M. Hydrogen storage properties of Pd nanoparticle/carbon template composites. *Carbon* **2008**, *46*, 206–214.
- (52) Sankaran, M.; Viswanathan, B. The role of heteroatoms in carbon nanotubes for hydrogen storage. *Carbon* **2006**, *44*, 2816–2821.
- (53) Zhang, Z.; Cho, K. Ab initio study of hydrogen interaction with pure and nitrogen-doped carbon nanotubes. *Phys. Rev. B* **2007**, *75*, 075420.
- (54) Srinivas, G.; Zhu, Y.; Piner, R.; Skipper, N.; Ellerby, M.; Ruoff, R. Synthesis of graphene-like nanosheets and their hydrogen adsorption capacity. *Carbon* **2010**, *48*, 630–635.
- (55) Subrahmanyam, K. S.; Vivekchand, S. R. C.; Govindaraj, A.; Rao, C. N. R. A study of graphenes prepared by different methods: characterization, properties and solubilization. *J. Mater. Chem.* **2008**, *18*, 1517–1523.
- (56) Banerjee, S.; Pillai, C. G. S.; Majumder, C. First-principles study of the H<sub>2</sub> interaction with transition metal (Ti, V, Ni) doped Mg(0001) surface: Implications for H-storage materials. *J. Chem. Phys.* **2008**, *129*, 174703–6.
- (57) Banerjee, S.; Pillai, C. G. S.; Majumder, C. Dissociation and Diffusion of Hydrogen on the Mg(0001) Surface: Catalytic Effect of V and Ni Double Substitution. *J. Phys. Chem. C* **2009**, *113*, 10574–10579.
- (58) Lee, H.; Ihm, J.; Cohen, M. L.; Louie, S. G. Calcium-Decorated Graphene-Based Nanostructures for Hydrogen Storage. *Nano Lett.* **2010**, *10*, 793–798.
- (59) Ao, Z. M.; Jiang, Q.; Zhang, R. Q.; Tan, T. T.; Li, S. Al doped graphene: A promising material for hydrogen storage at room temperature. *J. Appl. Phys.* **2009**, *105*, 074307–6.
- (60) López-Corral, I.; Germán, E. a.; Juan, A.; Volpe, M. a. A.; Brizuela, G. P. DFT Study of Hydrogen Adsorption on Palladium Decorated Graphene. *J. Phys. Chem. C* **2011**, *115*, 4315–4323.
- (61) Horinouchi, S.; Yamanoi, Y.; Yonezawa, T.; Moura, T.; Nishihara, H. Hydrogen Storage Properties of Isocyanide-Stabilized Palladium Nanoparticles. *Langmuir* **2006**, *22*, 1880–1884.
- (62) Kim, G.; Jhi, S.-H.; Park, N. Effective metal dispersion in pyridinolike nitrogen doped graphenes for hydrogen storage. *Appl. Phys. Lett.* **2008**, *92*, 013106–3.